Capturing CO_2 under Dry and Humid Conditions
When Does the Parent MOF Outperform the MTV MOF?

Huang, Chunyu; Noorian Najafabadi, Seyyed Abbas; Albertsma, Jelco; Rook, Willy; Fischer, Marcus; Hartmann, Martin; van der Veen, Monique Ann

DOI
10.1021/acs.inorgchem.5c02921

Publication date
2025

Document Version
Final published version

Published in
Inorganic chemistry

Inorganic Chemistry

pubs.acs.org/IC

Article

Capturing CO_2 under Dry and Humid Conditions: When Does the Parent MOF Outperform the MTV MOF?

Chunyu Huang, Seyyed Abbas Noorian Najafabadi, Jelco Albertsma, Willy Rook, Marcus Fischer, Martin Hartmann, and Monique Ann van der Veen*

Cite This: *Inorg. Chem.* 2025, 64, 18916−18924

Read Online

ACCESS | Metrics & More | Article Recommendations | Supporting Information

ABSTRACT: A key challenge in capturing CO_2 from postcombustion gases is humidity due to competitive adsorption between CO_2 and H_2O. Multivariate (MTV) metal−organic frameworks (MOFs) have been considered a promising option to address this problem, e.g., combining CO_2-affinitive and hydrophobic groups. Here, we synthesized a series of amine and methyl cofunctionalized MTV MIL-53(Al)-xNH$_2$(1 − x)CH$_3$ and their parent materials. All the mixed linker MIL-53(Al)-xNH$_2$(1 − x)CH$_3$ showed amino linker enrichment compared to the synthesis ratio, yet the linkers were distributed relatively homogeneously from the bulk to the surface. Material hydrophobicity or hydrophilicity varied with methyl or amino group content, respectively. The single-component adsorption indicated that certain mixed linker MIL-53(Al)-xNH$_2$(1 − x)CH$_3$ might outcompete the parent materials. In CO_2−H_2O competitive adsorption, however, the hydrophobic parental MIL-53(Al)−CH$_3$ outperformed the mixed linker MOFs. CO_2 adsorption capacities of 5.4, 4.9, and 3.6 wt % were found for 0.3 bar of CO_2 under 0, 5, and 10% RH, respectively. The results highlight that materials with enhanced hydrophobicity and tight-fitting pores can outperform groups with high CO_2 affinity in the CO_2 capture under humid conditions.

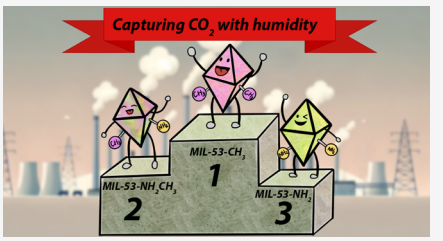

1. INTRODUCTION

Climate change has become one of the most intractable problems on the planet. One of the main culprits is carbon dioxide (CO_2), with an emission rate of more than 36 gigatons per year, posing an urgent need for capture and storage. About 45% of the CO_2 emissions originate from industries and power plants via fuel combustion.[1] Capturing CO_2 on solid adsorbents from the exhaust gas stream appears to be a promising alternative technology because it is more cost-effective, has a lower energy demand, and is noncorrosive compared to the conventional way of absorbing CO_2 by alkanolamine solutions.[2]

A variety of solid adsorbents have been explored for CO_2 adsorption in the last 20 years, such as zeolites, silicas, carbons, and metal−organic frameworks (MOFs). Among the candidates, MOFs have drawn growing attention because of their high porosities and chemical tailorability.[1] Depending on the specific industry fields, the postcombustion flue gases can contain 5−20 vol% of moisture.[3] If precondensation of water content can be avoided, the CO_2 capture process will be more energy-efficient, making it the key to identifying sorbents that can competitively adsorb CO_2 in the presence of water.[4,5] In some cases, cooperative H_2O−CO_2 adsorption was even reported, where adsorbed H_2O enhances CO_2 adsorption under specific relative humidity.[2] This type of adsorption leads to moisture-enhanced CO_2 capture, such as in NOTT-400,[6] NOTT-401,[7] MIL-53(Al),[8] and TAPB-NDA covalent organic framework (COF).[9] In these cases, moisture enhancement of CO_2 only occurs when a limited amount of water is adsorbed and no longer occurs at higher relative humidities where pore-filling water condensation has taken place. However, most frequently, competitive H_2O−CO_2 adsorption was observed in MOFs, where H_2O has a detrimental effect on CO_2 adsorption due to the large dipole moment and hydrogen bonding potential of H_2O molecules.[4] Alkyl amine-based MOFs do not suffer from H_2O−CO_2 competitive adsorption but exhibit a high heat of absorption (∼60 to 90 kJ/mol), which is excessive for point-source CO_2 capture. In contrast, MOF functionalized with aromatic amines presents lower CO_2 adsorption enthalpies (∼30 to 40 kJ/mol), enabling more energy-efficient regeneration.[10] However, aromatic amine-based MOFs do suffer from competitive H_2O adsorption. Zaráte and co-workers[11] investigated the influence of the amino group in MIL-53(Al)−NH$_2$ on CO_2 adsorption under humid conditions. The CO_2 capture ability of MIL-53(Al)−NH$_2$ decreased dramatically in comparison to MIL-53(Al) with an increase in relative humidity.

To address the challenge of CO_2−H_2O competitive adsorption, dedicated efforts have been put into the develop-

Received: June 26, 2025
Revised: July 29, 2025
Accepted: July 30, 2025
Published: September 10, 2025

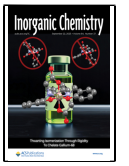

https://doi.org/10.1021/acs.inorgchem.5c02921
Inorg. Chem. 2025, 64, 18916−18924

Scheme 1. Synthesis of MIL-53(Al)-xNH$_2$(1 − x)CH$_3$

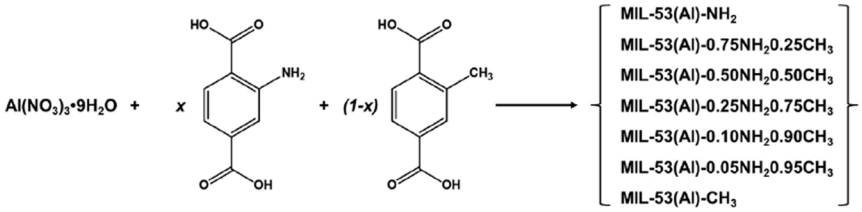

ment of multivariate MOFs (MTV-MOFs), where multifunctionalities, offered by different linkers, metals, or both, can be incorporated into MOF structures. Thus, MTV-MOFs can combine the merits of each parental MOF and have demonstrated synergistic effects.[12] For example, besides introducing CO_2-philic groups that suffer from competitive H_2O adsorption (e.g., aromatic−NH_2 and phenolic−OH groups), H_2O repellent groups (e.g., fluoridated, aliphatic groups) can also be introduced simultaneously into the structures. If the relative humidity at which pore-filling water condensation takes place can be increased by employing this strategy while at the same time retaining groups for CO_2 adsorption, then it could be very favorable. Hu et al.[13] synthesized a series of mixed linker UiO-66-NH_2−F_4, of which UiO-66-NH_2−F_4-0.53 can retain 70% of its CO_2 uptake capacity under 70% relative humidity at 298 K. On the other hand, UiO-66-NH_2 retained only 12% CO_2 of its uptake capacity under the same conditions. Similarly, Park et al.[14] synthesized bifunctionalized MIL-101(Cr)-NH_2−F-0.5. It was discovered that MIL-101(Cr)-NH_2−F-0.5 only lost 10% capacity for CO_2 at 303 K and 1 bar under 60% relative humidity, but the capacity was reduced by 40% for MIL-101(Cr)−NH_2. In these studies, however, the CO_2 capturing ability of the hydrophobic parental MOFs under humid conditions was not investigated. Nonetheless, it is necessary to include these results to answer whether developing MTV-MOFs with CO_2-philic groups and H_2O repellent groups is truly the best strategy for CO_2 capture under humid conditions.

Furthermore, only the bulk ratio of different components has generally been investigated in MTV-MOFs and not the spatial distribution, although this also influences the adsorption properties.[15] A homogeneous structure with various components distributed statistically is usually regarded as the default when a one-pot synthesis is carried out. In reality, however, due to different reactivities of the components affecting the crystallization kinetics, nonrandom structures might form (e.g., cluster domains, and core−shell).[16,17] Sometimes, even mixed-phase MOFs formed instead of mixed crystallites.[18] To sum up, the distribution of various components in the MOF crystals is desired for a deeper understanding in the current research.

We focus here on MIL-53 (MIL = Matriaux de l'Institut Lavoisier), an MOF composed of chains of [$MO_4(OH)_2$] polyhedra of inorganic trivalent metal ions (M = Al, Fe, Ga, Cr, and In) and terephthalate linkers,[19] resulting in one-dimensional diamond-shaped channels. Upon external stimulus, such as temperature, pressure, and/or guest molecule inclusion, the structure can undergo a reversible phase transition between a large pore (LP) form and a narrow pore (NP) form, the so-called "breathing effect." The breathing effect can also be influenced by the building blocks and particle size of the MOFs, such as the metal ions and the functionalization of linkers.[19−22] The combination of the breathing effect of MIL-53 and the mixed-linker strategy enables more possibilities for material design and applications.[23−28] Yang et al. synthesized a series of mixed linker MIL-53(Al)−OH_x.[26,27] The CO_2 adsorption capacities of MIL-53(Al)−OH_{25} and MIL-53(Al)−OH_{50} were approximately 19% higher than that of MIL-53(Al) under the same conditions. However, MIL-53(Al)−OH_{75} and MIL-53(Al)−OH_{100} exhibited much lower CO_2 uptake due to the introduction of hydroxyl groups on the organic linkers, which stabilized the NP form and made it more difficult for CO_2 to be absorbed. We report the first MTV-based MIL-53 in which both a functional group targeting CO_2 adsorption (namely, aromatic −NH_2) and a functional group enhancing hydrophobicity (namely, −CH_3) are incorporated. A series of mixed linker MIL-53(Al)-xNH$_2$(1 − x)CH$_3$ was synthesized, where x and (1 − x) represent the molar ratio of 2-amino terephthalic acid and 2-methyl terephthalic acid in the initial synthesis (x = 0, 0.05, 0.10, 0.25, 0.50, 0.75, and 1), respectively. We explicitly investigated the bulk and the surface concentration of the linker ratio as a measure of spatial distribution across the MOFs through a series of techniques (i.e., elemental analysis, ATR-IR, and XPS). We performed single-component CO_2 and H_2O adsorption, as well as evaluated the CO_2−H_2O coadsorption for the mixed-linker series and compared these not only to MIL-53(Al)-NH_2 but also to the hydrophobic parent MOF MIL-53(Al)−CH_3. Intriguingly, we found that the parental MIL-53(Al)−CH_3 outperformed the mixed linker MIL-53(Al)s to capture CO_2 under humid conditions.

2. EXPERIMENTAL SECTION

2.1. Chemicals and Reagents. Aluminum nitrate nonahydrate ($Al(NO_3)_3.9H_2O$) (>98%, Sigma-Aldrich), 2-aminoterephthalic acid (H_2BDC−NH_2) (99%, Thermo scientific), 2-methylterephthalic acid (H_2BDC−CH_3) (97%, Fluorochem), terephthalic acid (H_2BDC) (98%, Aldrich), N,N-dimethylformamide (DMF) (>99.9%, Sigma-Aldrich), and acetone (>99.5%, Honeywell) were used without further purification.

2.2. Synthesis of MIL-53(Al)-xNH$_2$(1 − x)CH$_3$. Two pure-linker samples, namely MIL-53-NH_2 and MIL-53-CH_3, and five mixed-linker samples MIL-53(Al)-xNH$_2$(1 − x)CH$_3$(x = 0.05, 0.10, 0.25, 0.50, 0.75, and 1) were synthesized based on the literature with some modifications (Scheme 1).[29]

Briefly, 2 mmol (0.7602 g) of $Al(NO_3)_3.9H_2O$ was dissolved in 5 mL of distilled water (solution A). Then, 3 mmol of two linkers was added, consisting of various ratios of 2-amino terephthalic acid (H_2BDC−NH_2) and 2-methyl terephthalic acid (H_2BDC−CH_3). The H_2BDC−NH_2 to H_2BDC−CH_3 ratio is 0−100% (0 mmol−3 mmol), 5−95% (0.15 mmol−2.85 mmol), 10−90% (0.3 mmol−2.7 mmol), 25−75% (0.75 mmol−2.25 mmol), 50−50% (1.5 mmol−1.5 mmol), 75−25% (2.25 mmol−0.75 mmol), and 100−0% (3 mmol−0 mmol). The linker(s) were added to 20 mL of DMF (solution B). Next, solutions A and B were combined into a 40 mL Teflon-lined autoclave and stirred at 150 rpm for 60 min on a magnetic stirrer plate. Afterward, the autoclaves were placed in an oven at 150 °C for 24 h.

After cooling down to room temperature, the products were washed with DMF three times in a centrifuge, dried in a vacuum oven

https://doi.org/10.1021/acs.inorgchem.5c02921
Inorg. Chem. 2025, 64, 18916−18924

at 60 °C for 24 h, and marked as as-synthesized samples. Subsequently, about 0.25 g of each product was boiled with 20 mL of DMF in 40 mL Teflon-lined autoclaves at 150 °C for 5 h to remove the unreacted linkers trapped in the pores. Finally, the products were activated by washing with acetone three times in a centrifuge and dried in a vacuum oven at 150 °C for 24 h. These samples are marked as activated samples. The masses of the activated MIL-53(Al)-xNH$_2$(1 − x)CH$_3$ samples are approximately as follows: 287 mg for MIL-53(Al)−CH$_3$, 250 mg for MIL-53(Al)-0.05NH$_2$0.95CH$_3$, 274 mg for MIL-53(Al)-0.10NH$_2$0.90CH$_3$, 259 mg for MIL-53(Al)-0.25NH$_2$0.75CH$_3$, 270 mg for MIL-53(Al)-0.50NH$_2$0.50CH$_3$, 274 mg for MIL-53(Al)-0.75NH$_2$0.25CH$_3$, and 260 mg for MIL-53(Al)-NH$_2$. The benchmark MIL-53(Al) was synthesized and activated using the same protocol mentioned earlier but using 3 mmol terephthalic acid as a linker. The mass of the activated MIL-53(Al) is about 240 mg.

3. RESULTS AND DISCUSSION

To confirm that MIL-53(Al) isostructures have been synthesized, powder X-ray diffraction (PXRD) was first performed on the MIL-53(Al)-xNH$_2$(1 − x)CH$_3$ series and MIL-53(Al). As shown in Figures 1 and S1, after activation, all

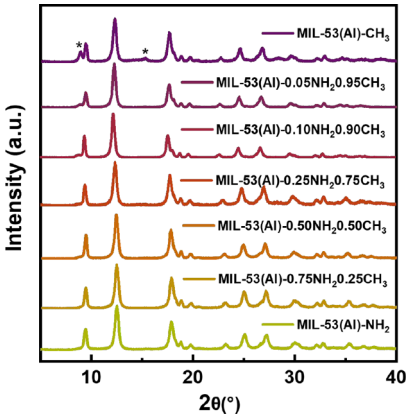

Figure 1. PXRD pattern of activated MIL-53(Al)-xNH$_2$(1 − x)CH$_3$ series. * corresponds to a diffraction peak of the large pore form.

MIL-53(Al)-xNH$_2$(1 − x)CH$_3$ and MIL-53(Al) exhibited the characteristic peaks of MIL-53 in a narrow pore form (2θ = 9.4 and 12.3°). Intriguingly, with an increasing amount of −CH$_3$ groups incorporated into the structures, two small shoulder peaks at 8.8 and 1 5° can be observed more obviously, which correspond to the large pore form of MIL-53. Crystal parameters of two mixed-linker MOFs (MIL-53(Al)-*0.75*NH$_2$*0.25*CH$_3$ and MIL-53(Al)-*0.05*NH$_2$*0.95*CH$_3$) were then obtained via 3D electron diffraction (Figure S2 and Table S1). The unit cell volume of the amino-rich material is smaller than that of the methyl-rich material due to the hydrogen bonding between −NH$_2$ groups and -μ(OH) in the organic chain, which is in line with the observations in the literature.[20,30] Thermogravimetric analysis (TGA) showed decent thermal stability of the materials. The materials do not collapse until 400−450 °C, depending on the ratio of −NH$_2$ and −CH$_3$ groups, which is in agreement with what has been reported in the literature.[30,31] Before the material decomposition, only a drop around 100 °C was observed due to the evaporation of water molecules, demonstrating that good activation was achieved, meaning no DMF or extra linkers were trapped inside the MOF pores (Figure S3). As shown in Figure 2A, no significant infrared absorption peaks related to free linkers (−COOH at 1680 cm^{-1}) or N,N-dimethylfomamide (e.g., C═O stretching at 1665 cm^{-1}) appeared, further substantiating proper activation. Scanning electron microscopy (SEM) revealed that the synthesized MIL-53(Al)-xNH$_2$(1 − x)CH$_3$ and MIL-53(Al) are highly agglomerated nanoparticles, with a size distribution between 100 and 140 nm (Figure S4), which is comparable to the crystal size reported in the literature when using DMF-water mixed solvents for the synthesis.[31]

The ratio and distribution of linkers in MTV-MOFs can greatly affect the properties of the materials.[15] Thus, attenuated total reflectance-infrared spectroscopy (ATR-IR), elemental analysis, and X-ray photoelectron spectroscopy (XPS) were employed to determine the overall ratio of the two linkers in the material as well as the ratio close to the external surface. As shown in Figure 2A, with the ratio varying between two linkers, relative intensity changes in several mid-IR absorption bands could be noticed. With the increasing amount of H$_2$BDC−NH$_2$ linkers used in the synthesis, bands stemming from N−H symmetric and asymmetric vibrations at 3499 and 3387 cm^{-1} and C−N stretching at 1255 cm^{-1} increased. On the other hand, when more H$_2$BDC−CH$_3$ linkers were incorporated into the structures, a weak band at 1209 cm^{-1} gradually appeared,

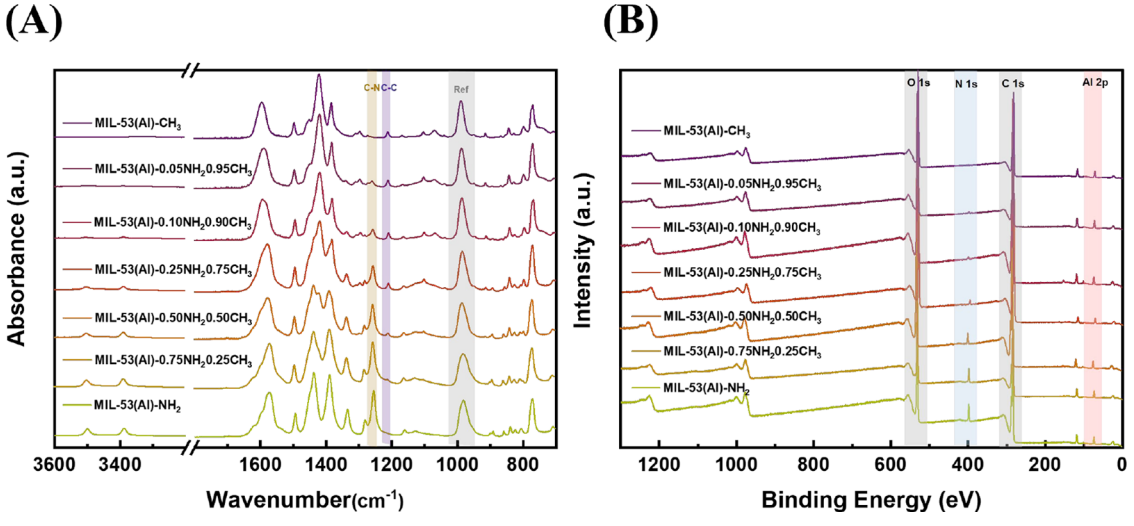

Figure 2. (A) ATR-IR spectra and (B) survey XPS scans on MIL-53(Al)-xNH$_2$-(1 − x)CH$_3$.

https://doi.org/10.1021/acs.inorgchem.5c02921
Inorg. Chem. 2025, 64, 18916−18924

which is due to the increasing presence of the methyl group. The penetration depth of the IR beam when using ZnSe is a few micrometers, meaning the IR beam can effectively penetrate the entire MOF crystals, which are only 100−140 nm in size. That allows us to combine the Lambert−Beer law and an internal reference peak (in this case, μ(OH) band located at 980−986 cm^{-1})[32] to calculate the average percentage of $H_2BDC-NH_2$ and/or $H_2BDC-CH_3$ in the bulk material from ATR-IR, as shown in Table 1 (for detailed calculation procedures using ATR-IR results, see Table S2). However, we mention that the most representative and separated band attributed to $H_2BDC-CH_3$ at 1209 cm^{-1} is rather weak, resulting in substantial inaccuracy when quantifying $H_2BDC-CH_3$, especially in samples with low CH_3 content using ATR-IR. To quantify the actual linker ratio in the crystals, we also employed elemental analysis to validate the $H_2BDC-NH_2$ and $H_2BDC-CH_3$ ratio (Tables 1 and S3). The atomic ratios of N:Al were utilized to calculate the linker ratios. Very interestingly, it is found that the amount of the two linkers in the final structure is different from the proportion of the initial ratio in the synthesis for all mixed linker MIL-53s. A greater amount of $H_2BDC-NH_2$ was incorporated into the structures compared to the synthesis ratio, indicating a higher reactivity of $H_2BDC-NH_2$ compared with $H_2BDC-CH_3$. To maintain the consistency of the paper and avoid confusion, we point out that the linker ratios indicated in the MOF names are the ratios in the synthesis rather than the ratios in the crystals. Next, to assess the homogeneity of the mixed linkers within MIL-53s, XPS was further performed to obtain surface information referring to depths of less than 10 nm.[33] As depicted in Figure 2B, the XPS survey spectra revealed that all of the samples contain C, O, and Al as expected. For the samples in the presence of $H_2BDC-NH_2$ linkers, N was also detected. Subsequently, high-resolution spectra of N 1s, Al 2p, C 1s, and O 1s spectra were deconvoluted, and their atomic percentages were calculated (Figure S5 and Table S4). Thus, the determined $H_2BDC-NH_2$ percentage from XPS closely resembles the values obtained from elemental analysis and ATR-IR, indicating at least from the center to the surface that the two linkers are distributed relatively homogeneously. Nevertheless, on a smaller scale, some degree of nonrandom heterogeneity or pure-linker crystals may still exist.

Table 1. Observed $-NH_2$ Ratios in Different MOFs via Elemental Analysis and ATR-IR and XPS Techniques

	$-NH_2$ ratio via elemental analysis (%)	observed $-NH_2$ via ATR-IR (%)	observed $-NH_2$ via XPS (%)
MIL-53-NH_2	100	100	100
MIL-53-0.75$NH_2$0.25CH_3	88	90	89
MIL-53-0.50$NH_2$0.50CH_3	63	75	72
MIL-53-0.25$NH_2$0.75CH_3	49	37	43
MIL-53-0.10$NH_2$0.90CH_3	18	16	14
MIL-53-0.05$NH_2$0.95CH_3	12	12	10
MIL-53-CH_3	0	0	0

The nitrogen adsorption isotherms on the different mixed-linker MIL-53 samples, the two parental MIL-53(Al)−CH_3 and MIL-53(Al)-NH_2, as well as MIL-53(Al) are shown in Figure 3A. The benchmark MIL-53(Al) displayed a type I isotherm. However, MIL-53-CH_3, MIL-53-NH_2, and mixed linker MIL-53(Al)-$x$$NH_2$-(1 − x)CH_3 showed an "S"-shaped adsorption isotherms, which is caused by an NP to LP transition.[25,30,34] The inflection point of the mixed linker MIL-53s is shifted compared to those of the parental MIL-53(Al)−CH_3 and MIL-53(Al)-NH_2 (Table S5). Moreover, the mixed linker MIL-53 did not behave as a linear combination of the parent MOFs, which indicates the incorporation of both linkers into the same crystals, as shown in Figure S6.

CO_2 adsorption was then carried out to assess the CO_2 capacity of each MOF (Figure 3B), and individual CO_2 adsorption−desorption curves are plotted in Figure S9). No phase transition was observed in either MIL-53(Al) or MIL-53(Al)-$x$$NH_2$(1 − x)CH_3 during CO_2 adsorption at 1.2 bar and 298 K. For MIL-53(Al), a potential low-pressure breathing behavior (LP−NP−LP) can occur below 1 bar, but this transition is highly dependent on crystal size.[35] In our case, the crystals were too small to exhibit this transformation.[21,22] For MIL-53(Al)-$x$$NH_2$(1 − x)CH_3, a pressure-induced transition from the NP to LP form may occur at higher CO_2 pressures, but the applied pressure (1.2 bar) remained below the threshold required to trigger such a change.[36,37] Overall, the introduction of the $-NH_2$ group presented a positive impact in increasing the total CO_2 capacity. Specifically, at 1.2 bar, MIL-

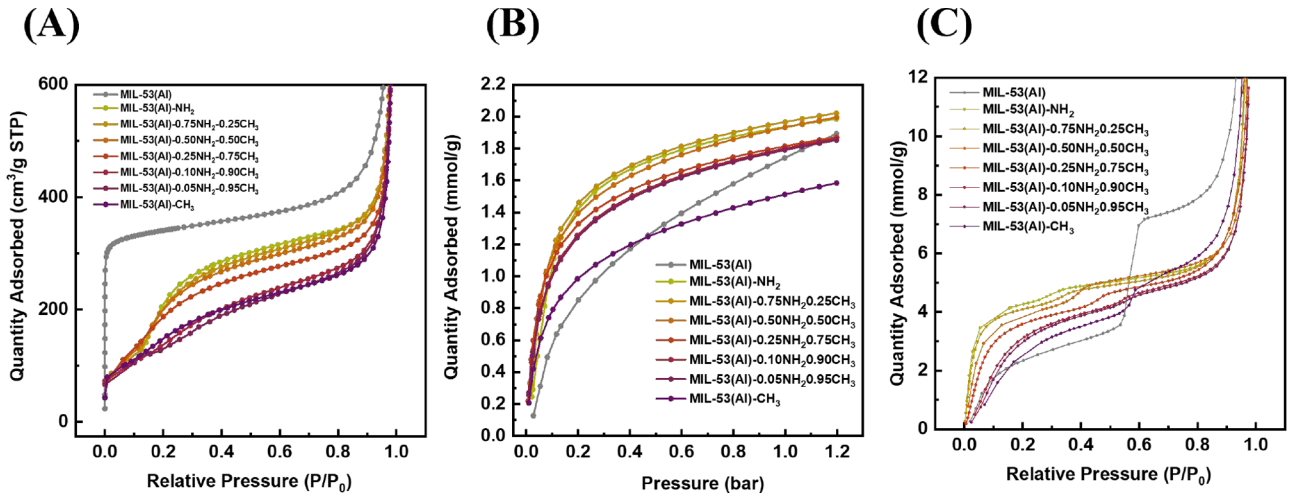

Figure 3. (A) N_2 adsorption at 77K, (B) CO_2 adsorption at 298 K, and (C) H_2O adsorption at 293 K on MIL-53(Al) and MIL-53(Al)-$x$$NH_2$(1 − x)CH_3.

https://doi.org/10.1021/acs.inorgchem.5c02921
Inorg. Chem. 2025, 64, 18916−18924

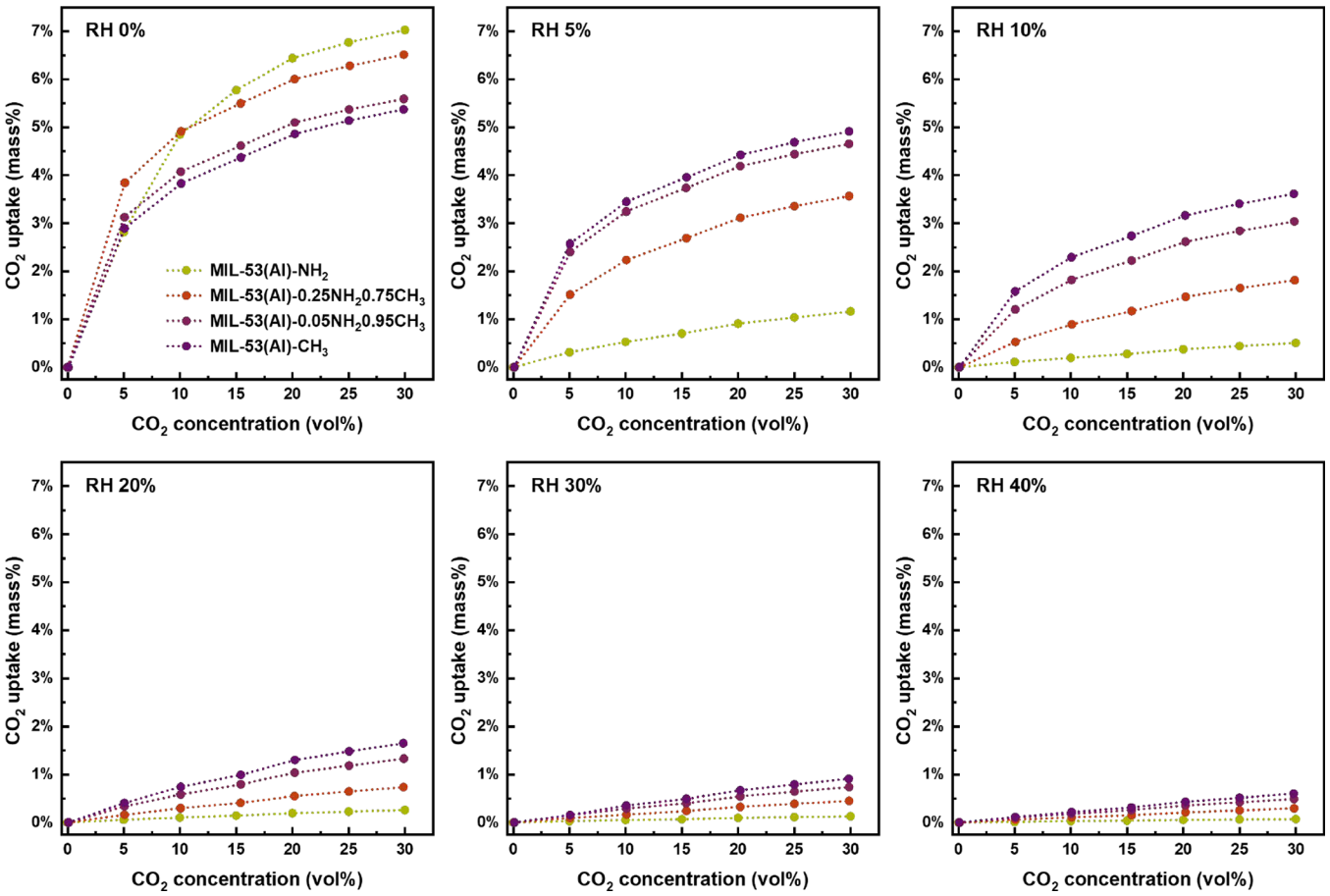

Figure 4. Mass change attributed to CO_2 uptake under 0, 5, 10, 20, 30, and 40% RH at 298 K on MIL-53(Al)−NH_2, MIL-53(Al)-0.25$NH_2$0.75CH_3, MIL-53(Al)-0.05$NH_2$0.95CH_3, and MIL-53(Al)−CH_3. The dashed lines were added for eye guidance.

53(Al)-0.75$NH_2$0.25CH_3 exhibited a CO_2 capacity of 2.02 mmol/g (~0.45 CO_2 per Al(OH)(X-terepthalate)), which is slightly higher than that of MIL-53(Al)-NH_2 (1.98 mmol/g, ~0.44 CO_2 per Al(OH)(X-terepthalate), and higher than that of MIL-53(Al)−CH_3 (1.58 mmol/g, ~0.35 CO_2 per Al(OH)-(X-terepthalate)), and MIL-53(Al) (1.89 mmol/g, ~0.39 CO_2 per Al(OH)(X-terepthalate)). Notice that 0.5 CO_2 per Al(OH)(X-terepthalate) means that one CO_2 molecule sits in one diamond-shaped window of four linkers in the NP form.[36] This is in line with earlier findings that much higher CO_2 partial pressures are required to transform MIL-53 or MIL-53−NH_2 into the LP form and thereby utilize their full adsorption capacity.[38] Intriguingly, up to 0.05 bar, MIL-53(Al)−CH_3 had a higher CO_2 uptake than MIL-53(Al)-NH_2; Up to 0.08 bar, all mixed-linker MIL-53(Al)-$x$$NH_2$$(1-x)$$CH_3$ displayed a higher absorption than MIL-53(Al)-NH_2; Up to 0.13 bar, MIL-53(Al)-0.50$NH_2$0.50CH_3 and MIL-53(Al)-0.75$NH_2$0.25CH_3 exhibited greater adsorption than MIL-53(Al)-NH_2, as shown in Figure S7. This phenomenon may be attributed to the introduction of $-CH_3$ groups slightly expanding the unit cell, yet leading to a smaller free pore diameter, making a more snug fit for CO_2, and thus stronger CO_2 adsorption. Yet, with pressure increasing, the CO_2 adsorbed among MIL-53(Al)-0.25$NH_2$0.75CH_3, MIL-53(Al)-0.10$NH_2$0.90CH_3, and MIL-53(Al)-0.05$NH_2$0.95CH_3 became similar, attaining 1.2 mmol/g at 1.2 bar. Similarly, the amount of CO_2 adsorbed by two amino-rich mixed-linker MOFs (MIL-53(Al)-0.75$NH_2$0.25CH_3 and MIL-53(Al)-0.50$NH_2$0.50CH_3), and MIL-53(Al)-NH_2, all reached approximately 2 mmol/g at 1.2 bar. This leads to the finding that there is a nonlinear relationship between the $-NH_2$ amount in crystals and the CO_2 capacity, meaning the isotherms of mixed linker MIL-53(Al)-$x$$NH_2$$(1-x)$$CH_3$ are not a weighted superposition of individual isotherms of the parental MOFs based on the linker proportions in the crystals, same as in N_2 adsorption (see calculated CO_2 adsorption isotherms in Figure S8).

Another striking observation is that MIL-53(Al)−CH_3 also showed slightly higher CO_2 uptake in comparison with MIL-53(Al) below 0.4 bar. We hypothesize that additional methyl groups inside the pores might decrease the free pore diameter, which increased van der Waals interactions without compromising the Coulombic interactions.[39,40] All in all, this suggests that a higher concentration of $-NH_2$ groups within the pores does not necessarily result in superior materials in terms of CO_2 capturing ability.

Next, to understand the hydrophobicity/hydrophilicity change with the variance of H_2BDC−NH_2 and H_2BDC−CH_3 linkers, we performed water adsorption measurements on the materials (Figure 3C), and for individual water adsorption isotherms, see Figure S10). The large additional water uptake for P/P_0 > 0.8 is due to water condensation in the voids between the MOF particles and is excluded from further discussion here. The benchmark MIL-53(Al) displays a type IV isotherm. Water is absorbed up to 3.4 mmol/g at 0.5 P/P_0 (~0.70 H_2O per Al(OH)(X-terephtalate)), followed by a sudden uptake to 7.1 mmol/g (~1.49 H_2O per Al(OH)(X-

https://doi.org/10.1021/acs.inorgchem.5c02921
Inorg. Chem. 2025, 64, 18916−18924

terephtalate)) around 0.6 P/P_0. This step corresponds to a phase transition from NP to LP form, which is in line with what has been reported previously when the MIL-53(Al) was synthesized in DMF.[41−43] In contrast, all MIL-53(Al)-xNH$_2$(1 − x)CH$_3$ showed a substantially lower uptake compared to that of MIL-53(Al) at 0.8 P/P_0, indicating that the introduction of functional groups stabilized the structures in the NP form during the water adsorption process. Water molecules filled up the pores in the low-pressure region up to 4.5 mmol/g for MIL-53(Al)-NH$_2$, followed by a small second step between 0.25 and 0.55 P/P_0 with an uptake of 4.87 mmol/g (1.09 H$_2$O per Al(OH)(X-terephtalate)), which is comparable to the reported water adsorption capacity of MIL-53(Al)−NH$_2$ by Yamada et al.[43] As expected due to the nature of the functional groups, MIL-53(Al)−CH$_3$ and MIL-53(Al)−NH$_2$ are the most hydrophobic and hydrophilic materials, respectively, in terms of the initial slope of the water adsorption isotherm and total water uptake. The mixed linker MIL-53(Al)-xNH$_2$(1 − x)CH$_3$ shows transient isotherms between the two parental materials; the more the −CH$_3$ groups are incorporated into the structures, the more hydrophobic the materials become, and *vice versa*.

As the CO$_2$ adsorption capacity is only impacted by a decrease in −NH$_2$ content to a limit (even with up to 95% −CH$_3$ in the synthesis), while the material does get more hydrophobic with increasing −CH$_3$ content, we expect that certain ratios of −CH$_3$/−NH$_2$ mixed linker MIL-53 will have a higher CO$_2$ adsorption under humid conditions compared to the parent materials, especially those with high −CH$_3$ content. Therefore, competitive CO$_2$−H$_2$O adsorption measurements were performed on the two pure-linker MOFs (MIL-53(Al)−NH$_2$ and MIL-53(Al)−CH$_3$), and two mixed-linker MOFs (MIL-53(Al)-0.05NH$_2$0.95CH$_3$ and MIL-53(Al)-0.25NH$_2$0.75CH$_3$). After being dried in situ, the materials were first equilibrated at certain relative humidities, and then experienced a CO$_2$ adsorption−desorption cycle at 298 K (for kinetic data, please see Figures S11−S14). The weight change between the prehumidified sample and after CO$_2$ loading was then considered as CO$_2$ being adsorbed, assuming that CO$_2$ did not desorb the preloaded water. Then, the uptake of CO$_2$ with exposure to different humidity can be calculated using eq 1, where $M_{CO_2+H_2O}$ represents the equilibrated weight after uptaking CO$_2$ and H$_2$O, M_{H_2O} represents the equilibrated weight after uptaking H$_2$O, and M_0 is the weight of the dried material.

$$\text{CO}_2\ \text{uptake (mass \%)} = \frac{M_{CO_2+H_2O} - M_{H_2O}}{M_0} \quad (1)$$

As shown in Figure 4, it can be noticed that under dry conditions, MIL-53(Al)-NH$_2$ has the highest CO$_2$ uptake when CO$_2$ concentration is higher than 5 vol %, whereas the other three materials had better performance at 5 vol %, which is also well in line with the results from volumetrically measured CO$_2$ adsorption isotherms, displayed in Figures 3A and S7. At 5% relative humidity and 30 vol % CO$_2$, MIL-53(Al)-NH$_2$ already lost 82% of its original adsorption capacity. In fact, for all measured relative humidity (RH), the higher the −CH$_3$ content, the higher the CO$_2$ adsorption, meaning that MIL-53(Al)−CH$_3$ outperformed all mixed-linker materials for all humidities. At 5 and 10% RH, in the presence of 30 vol % CO$_2$, MIL-53(Al)−CH$_3$ retains ∼91 and ∼65% of its original CO$_2$ adsorption capacity, respectively. For higher relative humidities, the CO$_2$ adsorption capacity quickly deteriorates for all materials. The mixed-linker MOFs show transient behavior between the two parent materials: under 5% RH and 30 vol % CO$_2$, 55 and 72% capacity were still remained for MIL-53(Al)-0.25NH$_2$0.75CH$_3$ and MIL-53(Al)-0.05NH$_2$0.95CH$_3$, respectively. In fact, for MIL-53(Al)−CH$_3$, quite significant CO$_2$ adsorption capacities of 4.9 and 3.6 wt % were found for 30 vol % CO$_2$ and 5 and 10% RH, respectively. This shows that −NH$_2$ groups in the structures had a negative impact on capturing CO$_2$ under humid conditions, implying that H$_2$O molecules had a stronger affinity than CO$_2$ to competitively bond with −NH$_2$ sites, which is consistent with the findings of Zárate et al.[11] Sánchez−Serratos et al. have reported the CO$_2$−H$_2$O competitive adsorption on MIL-53(Al), where a cooperative CO$_2$−H$_2$O adsorption was observed.[8] They discovered a 1.5-fold CO$_2$ adsorption increase, up to 5.2 wt % under 20% RH at 30 °C compared with dry CO$_2$.

We also expect that introducing hydrophobic groups, e.g., fluorine groups, into MIL-53(Al) may help mitigate water interference during CO$_2$ capture. Based on the water adsorption results of MIL-53(Al)-F$_2$ reported by Van Der Voort and co-workers[44] and that of MIL-53(Al)-F$_4$ reported by Guiotto et al.,[45] the steep water uptake step corresponding to water cluster formation is shifted to 50−70% RH upon fluorination, compared to ∼10% RH for MIL-53(Al). Therefore, it can be expected that the CO$_2$ adsorption capacity of MIL-53(Al)-Fx would be affected by water vapor only to a very limited extent prior to the pore-filling step. The strong CO$_2$ adsorption in MIL-53(Al)−CH$_3$ is rationalized by the small pore size in the NP form of this MOF. A similar strong CO$_2$ adsorption in MIL-53(Al)-Fx will thus depend on the structure remaining in the NP form under the relevant conditions. A caveat, however, is that compounds containing fluorinated carbon are under increased scrutiny due to their bioaccumulation and persistence in the environment due to the high stability of the fluorine-carbon bond. In summary, the competitive CO$_2$−H$_2$O adsorption behavior highlighted the importance of enhancing the hydrophobicity of adsorbents for carbon capture in the presence of water. It underscores for MTV-MOFs that a proper comparison with the parent MOFs is warranted.

4. CONCLUSIONS

In this study, a series of mixed linker MIL-53(Al)-xNH$_2$(1 − x)CH$_3$ and two parental materials were prepared successfully. With a combination of techniques, not only the bulk ratio but also the average spatial arrangement of BDC−NH$_2$ and BDC−CH$_3$ were studied. It is found that the actual ratios of BDC−NH$_2$ in mixed-linker MOFs were much higher than the initial ratio in the synthesis, indicating a higher reactivity of BDC−NH$_2$ compared to BDC−CH$_3$. By comparing the bulk ratio and surface ratio of the two linkers, we also confirmed a relatively homogeneous linker distribution from core to surface.

For all competitive and single-component CO$_2$ and H$_2$O adsorption measurements (up to 1.2 bar of CO$_2$ and 95% RH), the mixed linker MIL-53(Al)-xNH$_2$(1 − x)CH$_3$ and two parental materials remained in the NP form. For single-component CO$_2$ adsorption, amino groups overall showed a positive impact on increasing the CO$_2$ adsorption capacity. Among the materials, MIL-53(Al)-0.75NH$_2$0.25CH$_3$ exhibited the highest CO$_2$ uptake of 2.02 mmol/g at 1.2 bar at 298 K.

https://doi.org/10.1021/acs.inorgchem.5c02921
Inorg. Chem. 2025, 64, 18916−18924

However, the increase in CO_2 uptake is more than linear to the actual number of amino groups in the crystals. The single-component water adsorption isotherms at 293 K indicated that the introduction of methyl groups could effectively postpone the H_2O uptake to a higher RH, whereas the presence of amino groups made the materials more hydrophilic.

Based on the single-component adsorption behavior, the two mixed-linker MOFs most rich in CH_3 groups (MIL-53(Al)-0.05$NH_2$0.95CH_3 and MIL-53(Al)-0.25$NH_2$0.75CH_3) were judged to be most promising to examine the CO_2 uptake under humid conditions (RH = 5, 10, 20, 30, and 40%), and compared to the two parent MOFs. However, in the competitive adsorption of CO_2−H_2O, no synergetic effect between amino groups and methyl groups was observed. Under the tested RH range, the CO_2 adsorption for all MOFs decreased compared to dry conditions. Surprisingly, the hydrophobic parental MIL-53(Al)−CH_3 outperformed the mixed linker MIL-53(Al)-$x$$NH_2$$(1 - x)$$CH_3$ in terms of the capture of CO_2 under moist conditions. Notably, considerable CO_2 adsorption capacities of 4.9 and 3.6 wt % were observed under conditions of 30 vol % CO_2 with 5 and 10% RH, respectively.

Although tremendous research efforts have been dedicated to developing MTV-MOFs for the purpose of capturing CO_2 under humid conditions, so far, none of them have compared the MTV-MOFs with the hydrophobic parental one. The results here, however, demonstrate that the hydrophobic parental MOF can have the best performance to capture CO_2 under humid conditions and should thus be included in future studies. The work highlights that materials with enhanced hydrophobicity and tight-fitting pores rather than hydrophilic groups can be good. Sometimes, for CO_2 capture under humid conditions the hydrophobic material even outperforms materials with specific sites with high CO_2 affinity, due to their hydrophilicity. We hope that this study will help steer the direction of material development in this regard.

■ ASSOCIATED CONTENT

Supporting Information

The Supporting Information is available free of charge at https://pubs.acs.org/doi/10.1021/acs.inorgchem.5c02921.

Experimental details, materials, and characterizations of the materials, including TGA, SEM, IR, XPS, N_2, H_2O, and CO_2 adsorption isotherms and competitive CO_2−H_2O adsorption data (PDF)

■ AUTHOR INFORMATION

Corresponding Author

Monique Ann van der Veen − *Chemical Engineering Department, Delft University of Technology, 2629 HZ Delft, The Netherlands;* orcid.org/0000-0002-0316-4639; Phone: +31 15 2786458; Email: m.a.vanderveen@tudelft.nl

Authors

Chunyu Huang − *Chemical Engineering Department, Delft University of Technology, 2629 HZ Delft, The Netherlands;* orcid.org/0000-0002-2280-3766

Seyyed Abbas Noorian Najafabadi − *Chemical Engineering Department, Delft University of Technology, 2629 HZ Delft, The Netherlands; Department of Chemical Sciences, University of Padova, 35131 Padova, Italy;* orcid.org/0000-0002-8184-236X

Jelco Albertsma − *Chemical Engineering Department, Delft University of Technology, 2629 HZ Delft, The Netherlands;* orcid.org/0000-0002-1842-8406

Willy Rook − *Chemical Engineering Department, Delft University of Technology, 2629 HZ Delft, The Netherlands*

Marcus Fischer − *Erlangen Center for Interface Research and Catalysis (ECRC), Friedrich-Alexander-Universität Erlangen-Nürnberg (FAU), 91058 Erlangen, Germany*

Martin Hartmann − *Erlangen Center for Interface Research and Catalysis (ECRC), Friedrich-Alexander-Universität Erlangen-Nürnberg (FAU), 91058 Erlangen, Germany*

Complete contact information is available at: https://pubs.acs.org/10.1021/acs.inorgchem.5c02921

Author Contributions

C.H.: Conceptualisation, Methodology, Data curation, Formal analysis, Validation, Visualization, and Writing − original draft. S.A.N.N.: Data curation, Investigation. J.A.: Data curation, Formal analysis. W.R.:Formal analysis, Investigation, methodology. M.F.: Resources, Methodology, Data curation, Validation. M.H.: Resources, Methodology, Writing - review and editing. M.A.V.D.V.: Conceptualisation, Methodology, Funding acquisition, Supervision, Resources, and Writing − review and editing.

Funding

This project has received funding from the research program Nationale Wetenschapsagenda−Onderzoek op Routes door Consortia (NWA-ORC) 2020/21, which is (partly)financed by the Dutch Research Council (NWO) under number NWA.1389.20.123. S.A.N.N. acknowledges that results incorporated in this standard have received funding from the European Union Horizon Europe research and innovation program under the Marie Skodowska-Curie Action for the project n101107269 (ENLIVEN project).

Notes

The authors declare the following competing financial interest(s): Raw data can be found on 4TU dataset doi.org/10.4121/9952bbfe-5207-46ac-9d59-544d8e9224c3.

■ ACKNOWLEDGMENTS

Dr. Khai-Nghi TRUONG from Rigaku Europe SE is thanked for determining the crystal structures via 3D-ED.

■ REFERENCES

(1) Pardakhti, M.; Jafari, T.; Tobin, Z.; Dutta, B.; Moharreri, E.; Shemshaki, N. S.; Suib, S.; Srivastava, R. Trends in Solid Adsorbent Materials Development for CO2 Capture. *ACS Appl. Mater. Interfaces* **2019**, *11*, 34533−34559.

(2) Kolle, J. M.; Fayaz, M.; Sayari, A. Understanding the Effect of Water on CO $_2$ Adsorption. *Chem. Rev.* **2021**, *121*, 7280−7345.

(3) Gorbounov, M.; Halloran, P.; Masoudi Soltani, S. Hydrophobic and hydrophilic functional groups and their impact on physical adsorption of CO2 in presence of H2O: A critical review. *Journal of CO2 Utilization* **2024**, *86*, No. 102908.

(4) Rajendran, A.; Shimizu, G. K. H.; Woo, T. K. The Challenge of Water Competition in Physical Adsorption of CO2 by Porous Solids for Carbon Capture Applications−A Short Perspective. *Adv. Mater.* **2024**, *36*, No. 2301730.

(5) Chanut, N.; Bourrelly, S.; Kuchta, B.; Serre, C.; Chang, J.-S.; Wright, P. A.; Llewellyn, P. L. Screening the Effect of Water Vapour on Gas Adsorption Performance: Application to CO2 Capture from

Flue Gas in Metal−Organic Frameworks. *ChemSusChem* **2017**, *10*, 1543−1553.
(6) Álvarez, J. R.; Peralta, R. A.; Balmaseda, J.; González-Zamora, E.; Ibarra, I. A. Water adsorption properties of a Sc(III) porous coordination polymer for CO2 capture applications. *Inorganic Chemistry Frontiers* **2015**, *2*, 1080−1084.
(7) Lara-García, H. A.; Gonzalez, M. R.; González-Estefan, J. H.; Sánchez-Camacho, P.; Lima, E.; Ibarra, I. A. Removal of CO2 from CH4 and CO2 capture in the presence of H2O vapour in NOTT-401. *Inorganic Chemistry Frontiers* **2015**, *2*, 442−447.
(8) Sánchez-Serratos, M.; Bayliss, P. A.; Peralta, R. A.; González-Zamora, E.; Lima, E.; Ibarra, I. A. CO2 capture in the presence of water vapour in MIL-53(Al). *New J. Chem.* **2016**, *40*, 68−72.
(9) Veldhuizen, H.; Butt, S. A.; van Leuken, A.; van der Linden, B.; Rook, W.; van der Zwaag, S.; van der Veen, M. A. Competitive and Cooperative CO2−H2O Adsorption through Humidity Control in a Polyimide Covalent Organic Framework. *ACS Appl. Mater. Interfaces* **2023**, *15*, 29186−29194.
(10) Darunte, L. A.; Walton, K. S.; Sholl, D. S.; Jones, C. W. CO2 capture via adsorption in amine-functionalized sorbents. *Current Opinion in Chemical Engineering* **2016**, *12*, 82−90.
(11) Zárate, A.; Peralta, R. A.; Bayliss, P. A.; Howie, R.; Sánchez-Serratos, M.; Carmona-Monroy, P.; Solis-Ibarra, D.; González-Zamora, E.; Ibarra, I. A. CO_2 capture under humid conditions in NH_2-MIL-53(Al): the influence of the amine functional group. *RSC Adv.* **2016**, *6*, 9978−9983.
(12) Deng, H.; Doonan, C. J.; Furukawa, H.; Ferreira, R. B.; Towne, J.; Knobler, C. B.; Wang, B.; Yaghi, O. M. Multiple Functional Groups of Varying Ratios in Metal-Organic Frameworks. *Science* **2010**, *327*, 846−850.
(13) Hu, Z.; Gami, A.; Wang, Y.; Zhao, D. A Triphasic Modulated Hydrothermal Approach for the Synthesis of Multivariate Metal−Organic Frameworks with Hydrophobic Moieties for Highly Efficient Moisture-Resistant CO2 Capture. *Adv. Sustainable Syst.* **2017**, *1*, No. 1700092.
(14) Park, J. M.; Cha, G.-Y.; Jo, D.; Cho, K. H.; Yoon, J. W.; Hwang, Y. K.; Lee, S.-K.; Lee, U.-H. Amine and fluorine co-functionalized MIL-101(Cr) synthesized via a mixed-ligand strategy for CO2 capture under humid conditions. *Chemical Engineering Journal* **2022**, *444*, No. 136476.
(15) Canossa, S.; Ji, Z.; Gropp, C.; Rong, Z.; Ploetz, E.; Wuttke, S.; Yaghi, O. M. System of sequences in multivariate reticular structures. *Nature Reviews Materials* **2023**, *8*, 331−340.
(16) Ragon, F.; Chevreau, H.; Devic, T.; Serre, C.; Horcajada, P. Impact of the Nature of the Organic Spacer on the Crystallization Kinetics of UiO-66(Zr)-Type MOFs. *Chem.—Eur. J.* **2015**, *21*, 7135−7143.
(17) Kubo, M.; Hagi, H.; Shimojima, A.; Okubo, T. Facile Synthesis of Hydroxy-Modified MOF-5 for Improving the Adsorption Capacity of Hydrogen by Lithium Doping. *Chem.− Asian J.* **2013**, *8*, 2801−2806.
(18) Schlüsener, C.; Jordan, D. N.; Xhinovci, M.; Matemb Ma Ntep, T. J.; Schmitz, A.; Giesen, B.; Janiak, C. Probing the limits of linker substitution in aluminum MOFs through water vapor sorption studies: mixed-MOFs instead of mixed-linker CAU-23 and MIL-160 materials. *Dalton Transactions* **2020**, *49*, 7373−7383.
(19) Millange, F.; Walton, R. I. MIL-53 and its Isoreticular Analogues: a Review of the Chemistry and Structure of a Prototypical Flexible Metal-Organic Framework. *Isr. J. Chem.* **2018**, *58*, 1019−1035.
(20) Munn, A. S.; Pillai, R. S.; Biswas, S.; Stock, N.; Maurin, G.; Walton, R. I. The flexibility of modified-linker MIL-53 materials. *Dalton Transactions* **2016**, *45*, 4162−4168.
(21) Bon, V.; Busov, N.; Senkovska, I.; Bönisch, N.; Abylgazina, L.; Khadiev, A.; Novikov, D.; Kaskel, S. The importance of crystal size for breathing kinetics in MIL-53 (Al). *Chem. Commun.* **2022**, *58*, 10492−10495.
(22) Ehrling, S.; Miura, H.; Senkovska, I.; Kaskel, S. From macro-to nanoscale: finite size effects on metal−organic framework switchability. *Trends in Chemistry* **2021**, *3*, 291−304.
(23) Marx, S.; Kleist, W.; Huang, J.; Maciejewski, M.; Baiker, A. Tuning functional sites and thermal stability of mixed-linker MOFs based on MIL-53(Al). *Dalton Transactions* **2010**, *39*, 3795.
(24) Lescouet, T.; Kockrick, E.; Bergeret, G.; Pera-Titus, M.; Aguado, S.; Farrusseng, D. Homogeneity of flexible metal−organic frameworks containing mixed linkers. *J. Mater. Chem.* **2012**, *22*, 10287.
(25) Pera-Titus, M.; Lescouet, T.; Aguado, S.; Farrusseng, D. Quantitative Characterization of Breathing upon Adsorption for a Series of Amino-Functionalized MIL-53. *J. Phys. Chem. C* **2012**, *116*, 9507−9516.
(26) Yang, J.; Yan, X.; Xue, T.; Liu, Y. Enhanced CO_2 adsorption on Al-MIL-53 by introducing hydroxyl groups into the framework. *RSC Adv.* **2016**, *6*, 55266−55271.
(27) Andonova, S.; Ivanova, E.; Yang, J.; Hadjiivanov, K. Adsorption Forms of CO_2 on MIL-53(Al) and MIL-53(Al)−OH_x As Revealed by FTIR Spectroscopy. *J. Phys. Chem. C* **2017**, *121*, 18665−18673.
(28) Tahmouresilerd, B.; Larson, P. J.; Unruh, D. K.; Cozzolino, A. F. Make room for iodine: systematic pore tuning of multivariate metal−organic frameworks for the catalytic oxidation of hydroquinones using hypervalent iodine. *Catalysis Science & Technology* **2018**, *8*, 4349−4357.
(29) Wu, G.; Jiang, M.; Zhang, T.; Jia, Z. Tunable Pervaporation Performance of Modified MIL-53(Al)-NH2/Poly(vinyl Alcohol) Mixed Matrix Membranes. *J. Membr. Sci.* **2016**, *507*, 72−80.
(30) Biswas, S.; Ahnfeldt, T.; Stock, N. New Functionalized Flexible Al-MIL-53-X (X = -Cl, -Br, -CH3, -NO2, -(OH)2) Solids: Syntheses, Characterization, Sorption, and Breathing Behavior. *Inorg. Chem.* **2011**, *50*, 9518−9526.
(31) Cheng, X.; Zhang, A.; Hou, K.; Liu, M.; Wang, Y.; Song, C.; Zhang, G.; Guo, X. Size- and morphology-controlled NH2-MIL-53(Al) prepared in DMF−water mixed solvents. *Dalton Transactions* **2013**, *42*, 13698.
(32) Hoffman, A. E. J.; Vanduyfhuys, L.; Nevjestić, I.; Wieme, J.; Rogge, S. M. J.; Depauw, H.; Van Der Voort, P.; Vrielinck, H.; Van Speybroeck, V. Elucidating the Vibrational Fingerprint of the Flexible Metal−Organic Framework MIL-53(Al) Using a Combined Experimental/Computational Approach. *J. Phys. Chem. C* **2018**, *122*, 2734−2746.
(33) Racz, A. S.; Menyhard, M. XPS depth profiling of nano-layers by a novel trial-and-error evaluation procedure. *Sci. Rep.* **2024**, *14*, 18497.
(34) Bitzer, J.; Heck, S.-L.; Kleist, W. Tailoring the breathing behavior of functionalized MIL-53(Al,M)-NH2 materials by using the mixed-metal concept. *Microporous Mesoporous Mater.* **2020**, *308*, No. 110329.
(35) Boutin, A.; Springuel-Huet, M.-A.; Nossov, A.; Gedeon, A.; Loiseau, T.; Volkringer, C.; Férey, G.; Coudert, F.-X.; Fuchs, A. H. Breathing transitions in MIL-53 (Al) metal-organic framework upon xenon adsorption. *Angew. Chem., Int. Ed.* **2009**, *48*, 8314−8317.
(36) Stavitski, E.; Pidko, E. A.; Couck, S.; Remy, T.; Hensen, E. J. M.; Weckhuysen, B. M.; Denayer, J.; Gascon, J.; Kapteijn, F. Complexity behind CO2 Capture on NH2-MIL-53(Al). *Langmuir* **2011**, *27*, 3970−3976.
(37) Couck, S.; Gobechiya, E.; Kirschhock, C. E. A.; Serra-Crespo, P.; Juan-Alcañiz, J.; MartinezJoaristi, A.; Stavitski, E.; Gascon, J.; Kapteijn, F.; Baron, G. V.; Denayer, J. F. M. Adsorption and Separation of Light Gases on an Amino-Functionalized Metal−Organic Framework: An Adsorption and In Situ XRD Study. *ChemSusChem* **2012**, *5*, 740−750.
(38) Kriesten, M.; Vargas Schmitz, J.; Siegel, J.; Smith, C. E.; Kaspereit, M.; Hartmann, M. Shaping of Flexible Metal-Organic Frameworks: Combining Macroscopic Stability and Framework Flexibility. *Eur. J. Inorg. Chem.* **2019**, *2019*, 4700−4709.
(39) Liu, H.; Zhao, Y.; Zhang, Z.; Nijem, N.; Chabal, Y. J.; Zeng, H.; Li, J. The Effect of Methyl Functionalization on Microporous Metal-

https://doi.org/10.1021/acs.inorgchem.5c02921
Inorg. Chem. 2025, 64, 18916−18924

Organic Frameworks' Capacity and Binding Energy for Carbon Dioxide Adsorption. *Adv. Funct. Mater.* **2011**, *21*, 4754−4762.
(40) Burtch, N. C.; Jasuja, H.; Dubbeldam, D.; Walton, K. S. Molecular-level Insight into Unusual Low Pressure CO2 Affinity in Pillared Metal−Organic Frameworks. *J. Am. Chem. Soc.* **2013**, *135*, 7172−7180.
(41) Mounfield, W. P.; Walton, K. S. Effect of synthesis solvent on the breathing behavior of MIL-53(Al). *J. Colloid Interface Sci.* **2015**, *447*, 33−39.
(42) Han, B.; Chakraborty, A. Functionalization, protonation and ligand extension on MIL-53 (Al) MOFs to boost water adsorption and thermal energy storage for heat transformations. *Chemical Engineering Journal* **2023**, *472*, No. 145137.
(43) Yamada, T.; Shirai, Y.; Kitagawa, H. Synthesis, Water Adsorption, and Proton Conductivity of Solid-Solution-Type Metal−Organic Frameworks Al(OH)(bdc-OH)(bdc-NH2)1. *Chem.− Asian J.* **2014**, *9*, 1316−1320.
(44) Biswas, S.; Couck, S.; Denysenko, D.; Bhunia, A.; Grzywa, M.; Denayer, J. F.; Volkmer, D.; Janiak, C.; Van Der Voort, P. Sorption and breathing properties of difluorinated MIL-47 and Al-MIL-53 frameworks. *Microporous and mesoporous materials* **2013**, *181*, 175−181.
(45) Guiotto, V.; Notari, M. S.; Perego, J.; Morelli Venturi, D.; Nardelli, F.; Bordiga, S.et al.Tuning flexibility in Metal-Organic Frameworks via linker per-fluorination: revisiting the adsorption-induced breathing of MIL-53(Al). *ChemRxiv* 2025, , This content is a preprint and has not been peer-reviewed. https://pubs.rsc.org/en/content/articlelanding/2025/ta/d5ta04373e, peer-reviewed version

https://doi.org/10.1021/acs.inorgchem.5c02921
Inorg. Chem. 2025, 64, 18916−18924